

Received 17 July 2023, accepted 17 August 2023, date of publication 23 August 2023, date of current version 31 August 2023.

Digital Object Identifier 10.1109/ACCESS.2023.3308040

## RESEARCH ARTICLE

# Experimental Analysis of a New Low Power Wind Turbine Emulator Using a DC Machine and Advanced Method for Maximum Wind Power Capture

HAMZA BOUDJEMAI<sup>1</sup>, SID AHMED EL MEHDI ARDJOUN<sup>1,2</sup>, HOUCINE CHAFOUK<sup>2</sup>, MOULOUD DENAI<sup>3</sup>, ABDULAZIZ ALKUHAJLI<sup>4</sup>, (Member, IEEE), USAMA KHALED<sup>5</sup>, AND MOHAMED METWALLY MAHMOUD<sup>5</sup>

<sup>1</sup>IRECOM Laboratory, Faculty of Electrical Engineering, Djillali Liabes University, Sidi Bel-Abbes 22000, Algeria

<sup>2</sup>UNIROUEN, ESIGELEEC, IRSEEM, Normandy University, 76000 Rouen, France

<sup>3</sup>School of Physics, Engineering and Computer Science, University of Hertfordshire, AL10 9AB Hatfield, U.K.

<sup>4</sup>Electrical Engineering Department, College of Engineering, King Saud University, Riyadh 11421, Saudi Arabia

<sup>5</sup>Electrical Engineering Department, Faculty of Energy Engineering, Aswan University, Aswan 81528, Egypt

Corresponding authors: Sid Ahmed El Mehdi Ardjoun (elmehdi.ardjoun@univ-sba.dz) and Mohamed Metwally Mahmoud (metwally\_m@aswu.edu.eg)

This work was supported by the Researchers Supporting Project number (RSP2023R258), King Saud University, Riyadh, Saudi Arabia.

**ABSTRACT** This paper presents a new design of an experimental low power Wind Turbine Emulator (WTE) which has the advantage of being simple and easy to implement in practice. The proposed emulator takes into account the effect of Wind Turbine (WT) inertia as well as the nonlinearities in the system which make it suitable for all types of WTs. An efficient Maximum Power Point Tracking (MPPT) algorithm based on synergetic and backstepping nonlinear control theory has also been proposed to allow the WT to extract maximum power under a wide range of operating conditions. This is achieved by regulating the current at the input of the boost converter through these controllers. Furthermore, these nonlinear controllers considerably reduce the complexity of the design of the control scheme. Several experimental test are conducted to validate the MPPT strategy and the proposed control scheme using a dSPACE1104 board and MATLAB/Simulink environment, including different wind profiles and variable electrical load. The results obtained demonstrate the effectiveness of the designed WTE in reproducing the same mechanical behavior as the real turbine studied and the good performance achieved by the proposed MPPT control algorithm.

**INDEX TERMS** Wind turbine emulator, boost converter, MPPT, backstepping control, synergetic control, dSPACE1104.

## NOMENCLATURE

### A. LIST OF ACRONYMS

WT	Wind Turbine.
WTE	Wind Turbine Emulator.
SWT	Small Wind Turbine.
MPP	Maximum Power Point.
MPPT	Maximum Power Point Tracking.
OTC	Optimal Torque Control.
PSF	Power Signal Feedback.

TSR	Tip Speed Ratio.
P&O	Perturb and Observe.
DCM	Direct Current Motor.
DCG	Direct Current Generator.
PMSM	Permanent Magnet Synchronous Motor.
PMSG	Permanent Magnet Synchronous Generator.
FPGA	Field-Programmable Gate Array.
XSG	Xilinx System Generation.
FOC	Field-Oriented Control.
VFD	Variable-Frequency Drive.
IGBT	Insulated-Gate Bipolar Transistor.
IM	Induction Motor.

The associate editor coordinating the review of this manuscript and approving it for publication was N. Ramesh Babu<sup>1</sup>.

SC Synergetic Controller.  
 BC Backstepping Controller.

## B. LIST OF SYMBOLS

$P_t, P_{t\_opt}$	Mechanical and optimal power of the turbine.
$P_e$	Power at the terminals of the electric load.
$S$	Surface swept by the blades of the turbine.
$V_w V_w$	Wind speed upstream of the turbine.
$\rho$	Air density.
$C_p$	Power coefficient.
$\lambda$	Relative speed or speed ratio.
$R$	Radius of the turbine blades.
$\Omega \Omega_t, m$	Turbine and generator rotation speed.
$J_t$	Inertia of the turbine.
$f_t$	Coefficient of friction of the turbine.
$J_m$	Inertia of the generator.
$f_m f_m$	Coefficient of friction of the generator.
$T_e$	Electromagnetic torque of the generator.
$T_m$	Torque supplied by the turbine to the generator.
$J$	Total moment of inertia.
$f$	Total coefficient of friction.
$G$	Gearbox ratio.
$R_a$	Armature resistance.
$k$	Torque constant of the DC machine.
$d$	Duty cycle.

## I. INTRODUCTION

Wind energy has become, nowadays, one of the most promising renewable energy sources to reduce the dependence on fossil fuel resources and, their negative impact on the environment [1]. Wind energy conversion systems are complex, with nonlinear characteristics and subject to various external disturbances such as intermittent and variable wind speeds [2]. Therefore, conducting experiments on a real wind turbine required adequate installation and implied a high investment cost [3]. Having a wind turbine emulator capable of reproducing the static and dynamic characteristics of an actual wind turbine in real-time can be extremely useful to test and validate various control strategies for speed and torque regulation, maximum power extraction, etc. in wind energy conversion systems under different wind speed conditions.

Several WTEs have been discussed and developed. In the design of these emulators, the authors rely on several criteria, in particular: the motor drive and its control, power electronics converters, simulation software, and data acquisition boards. For example, in [4] the authors used a Direct Current Motor (DCM) with an armature current regulation loop based on a Proportional-Integral (PI) controller. This control structure is applied on a DC-DC buck converter using LabView software with Field-Programmable Gate Array (FPGA). In [5], the authors proposed a PI-based cascade control for the DCM (speed regulation in series with armature current regulation). This control is applied to a DC-DC

buck converter. The overall system and control scheme are modeled in MATLAB/Simulink and, then validated experimentally using a dSPACE1104 board. In [6], the authors used a similar system configuration, except that the cascade regulation is replaced by an armature current regulation loop based on a fuzzy controller, and the buck converter is replaced by a boost converter. The authors in [7], presented a new emulator slightly different from other emulators developed since it works in open-loop and without any feedback control signals. The emulator basically consists of a DCM driven by a buck converter. The DCM drive is controlled by the MATLAB/Xilinx System Generation (XSG) environment with the FPGA card. In [8], the DCM is replaced by a Permanent Magnet Synchronous Motor (PMSM) with a Field-Oriented Control (FOC) scheme based on PI controllers. etc.

This study builds upon the work presented in [9] where the authors proposed an emulator to mimic the mechanical behavior of a low power WT which operates without load. Hence, in this paper, a variable electrical load has been added to assess the WTE under more realistic conditions. Although, there are several WTEs available in the literature, the emulator proposed in this paper is different and offers more desirable features. In summary, the novelty of the proposed emulator can be summarized as follows:

- Simplicity of implementation: After a thorough search on WTEs, it has been noticed that for the electrical part of the WT system, several researchers [10], [11], [12], [13], [14] have used alongside the WTE very complex configurations (AC generator (PMSG, DFIG, etc.) – uncontrolled rectifier – filter – DC-DC converter – battery or electrical load) to perform tests on a DC load based on the control of a DC-DC converter. Unlike all these WTE configurations, our work aims to provide a simple experimental platform based only on DC machines to facilitate the study of Small WTs (SWTs). The proposed WTE is design to capture accurately the characteristics of real WTs. Thus, through this work, we do not encourage manufacturers to install Direct Current Generators (DCGs) in small WT chains like other researchers [15]. It is well known that this type of machine requires very expensive maintenance, without forgetting the commutation sparks on the machine collector due to load variation or machine shaft vibration, and with that, you can therefore imagine what would happen in case of turbulent wind facing a WT based on a DCG.
- The adaptation of the power between the wind turbine and the engine of the emulator, which is not considered in other emulators. In some of these WTEs, only the adaptation of current and/or torque is considered, and therefore for a given wind speed, the powers of the turbine and the motor drive of the emulator do not match. In some others, the motor rated power is greater than or equal to the rated power of the WT. In this paper, with a simple power adaptation technique, it was possible to

**TABLE 1. Comparative study of different WTE configurations.**

References	Machines used		Power electronics		Power adaptation	Effect of the inertia of the WT	Validation scenarios	
	Mechanical part	Electrical part	Mechanical part	Electrical part			Variable wind	Load effects
[6]	DCM	AC generator	• DC-DC Boost Converter	• No converter used • Capacitor bank	×	×	✓	×
[16]	IM Motor	PMSG	• Uncontrolled rectifier • Filter • 3 Phase IGBT Inverter	• Controllable rectifier • Filter • 3 Phase IGBT Inverter	×	✓	✓	×
[17]	IM Motor	PMSG	• VFD drive	• No converter used	×	✓	✓	×
[18]	DCM	PMSG	• DC drive	• Controllable rectifier • LC Filters • 3 Phase IGBT Inverter	×	×	✓	✓
[19]	DCM	PMSG	• Uncontrolled rectifier • Filter • DC-DC Buck Converter	• Uncontrolled rectifier • Filter	×	×	✓	×
[20]	DCM	PMSG	• DC-DC Buck Converter	• Uncontrolled rectifier • Filter • DC-DC Buck Converter	×	×	✓	×
This work	DCM	DCG	• DC-DC Buck Converter	• DC-DC Boost Converter	✓	✓	✓	✓

mimic the behavior of a WT, which has a nominal power of about fifteen times the nominal power of the emulator motor.

- Another advantage is that our emulator contains several electrical circuits in the form of modules, which greatly facilitates maintenance in the event of a breakdown or problem. Also according to the needs one can easily change the circuits, that is to say if one wants to test another control algorithm, it suffices to change the control circuit instead of completely changing the wind turbine emulator.
- Reasonable cost (simple power electronics circuit).
- As well, several research works propose wind turbine emulators, but without addressing neither the inertia effect of the turbine, nor its robustness against load variations. All these characteristics and features were considered in the design of the wind turbine emulator proposed in this work. The characteristics and performance of the proposed wind turbine emulator have been compared to other recent works in Table 1.

Despite the enormous environmental and economic benefits that the exploitation of wind energy systems brings, their integration into the electrical networks can be a challenge due to several factors such as the random variation of the wind profile or the variation of the electrical load. Several Maximum Power Point Tracking (MPpt) algorithms have been proposed to maximize the power captured by the WT and improve its efficiency. Among the MPPT techniques proposed in the literature, those in [11], [21], [22], and [23]

require an exact model of the WT such as for example; Power Signal Feedback (PSF), Optimal Torque Control (OTC), and Tip Speed Ratio (TSR). Other MPPT techniques which do not require any prior knowledge of WT parameters have also been proposed such as the Perturb & Observe (P&O) or based on fuzzy logic, control by the search for extremum, etc. This paper presents an MPPT based on Optimal Torque Control (OTC-MPpt). However, several authors who applied this technique to the mechanical part of the WT in their simulation studies did not address the effect of the inertia of the WT nor the effect of the variation of the electrical load. The WTE considered in this paper takes into account all these aspects. A simple control scheme based on nonlinear control theory is employed to force the WT to extract the maximum power from the wind regardless of the operating conditions. Among the different nonlinear control strategies that have received a lot of attention in recent years in various applications, we can mention synergistic control (SC) [28], [29], [30], [31] and backstepping control (BC) [32], [33], [34], [35]. Because these control techniques can be applied directly to the nonlinear model of the system to be controlled, in this work, we have chosen to use them alongside the OTC-MPPT to control a boost converter and improve the efficiency of the studied WTE.

The main objective behind developing a wind emulator is to facilitate the study of wind energy conversion systems and conduct real-time experiments to test and validate new control designs or power converter topologies under various operating conditions without the need to access real turbines

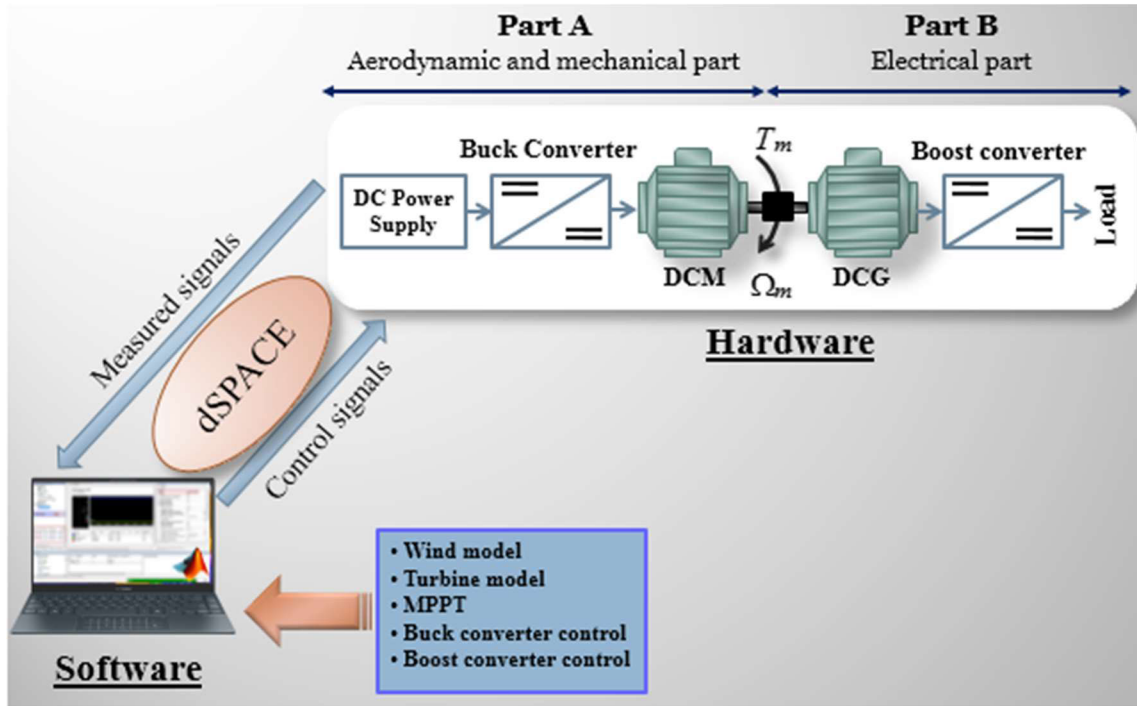


FIGURE 1. Block diagram of the proposed WTE.

which avoids the risk of damaging the actual system, saving time and increasing the quality of system development. As in our case, we used it to evaluate the feasibility of many MPPT techniques.

The remaining of the paper is organized as follows: Section II presents a detailed description of the main components of the proposed WTE. Section III presents the structure of the proposed OTC-MPPT and derive the equations of the nonlinear controllers. The validation scenarios and the discussion of the experimental results obtained are detailed in Section IV. Finally, the conclusion of the paper and the proposed future research works are summarized in Section V.

## II. MODELING OF THE WIND TURBINE EMULATOR

The WTE proposed in this paper for the study of SWTs is illustrated in Fig. 1. As mentioned earlier, this emulator is based on the work done in [9] (Part A). In this paper, we have designed Part B which consists of a DC Generator (DCG) followed by a boost converter and a variable electrical load. The WTE can be divided into two parts: Mechanical part and Electrical part not only expresses the mechanical part of the WT, but can be divided into two sub-emulators which are:

### A. MECHANICAL PART OF THE WTE

This part seeks to reproduce the mechanical behavior of the studied WT by controlling the DC motor. All the components of the turbine (the blades, the slow shaft, the gearbox, and the fast shaft) are modeled on MATLAB/Simulink software then implemented on the dSPACE1104 card in order to control a

Buck converter and generate the real WT torque signal, but at a reduced scale [9].

It is well known that when the wind blows, WTs can only capture part of the power of the wind which is given by the following relationship:

$$P_t = \frac{1}{2} \rho S V_w^3 C_p(\lambda) \quad (1)$$

The small power wind turbine used in this work is of the Darrieus type. This type of turbine rotates with a blade tip speed greater than the actual wind speed, so the relative speed  $\lambda$  is greater than 1. Thus, it uses the lift force to produce the rotation of the blades. It is well known that wind turbines using this type of force spin faster and are able to extract more power from the wind than those using drag force (ex: Savonius type turbine). Furthermore, because the energy conversion devices (generator, gearbox, power electronics, etc.) are placed at the foot of the wind turbine, it is easier to carry out maintenance operations. The main parameters of the turbine are summarized in Table 2, and the power coefficient of this turbine can be expressed by the following relationship [10]:

$$C_p(\lambda) = 0.00054\lambda^4 - 0.01098\lambda^3 + 0.057456\lambda^2 - 0.02493\lambda + 0.110898 \quad (2)$$

With

$$\lambda = \frac{R\Omega_t}{V_w} \quad (3)$$

Moreover, the mechanical power recovered by the WT (the slow shaft) is transmitted to the generator (the fast shaft) from

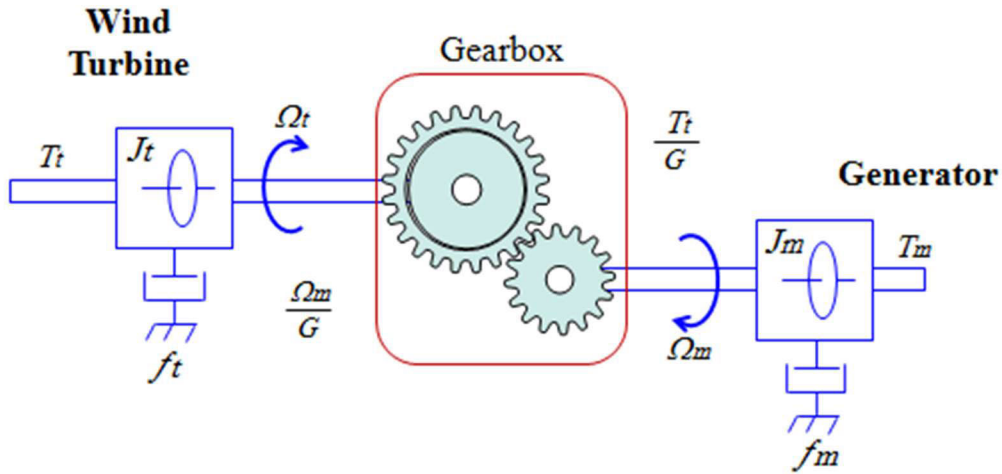


FIGURE 2. Mechanical coupling between WT and generator.

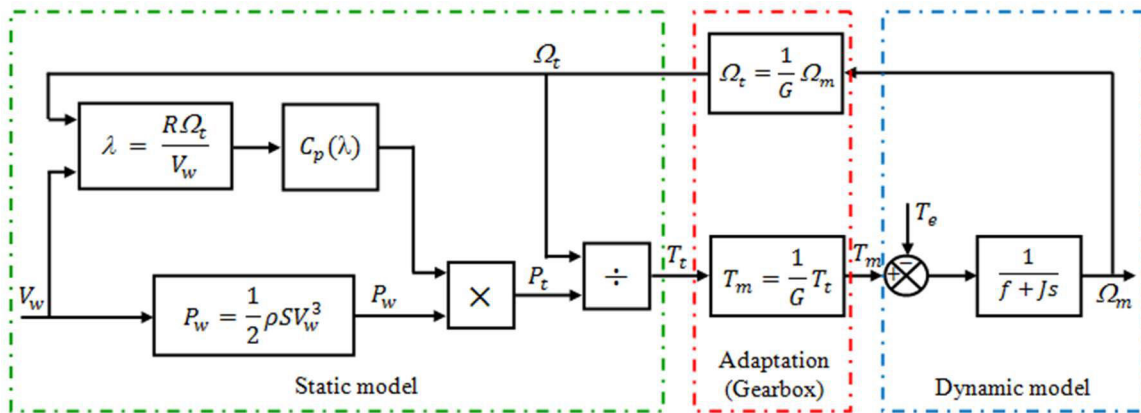


FIGURE 3. Schematic diagram of the principle of WTs.

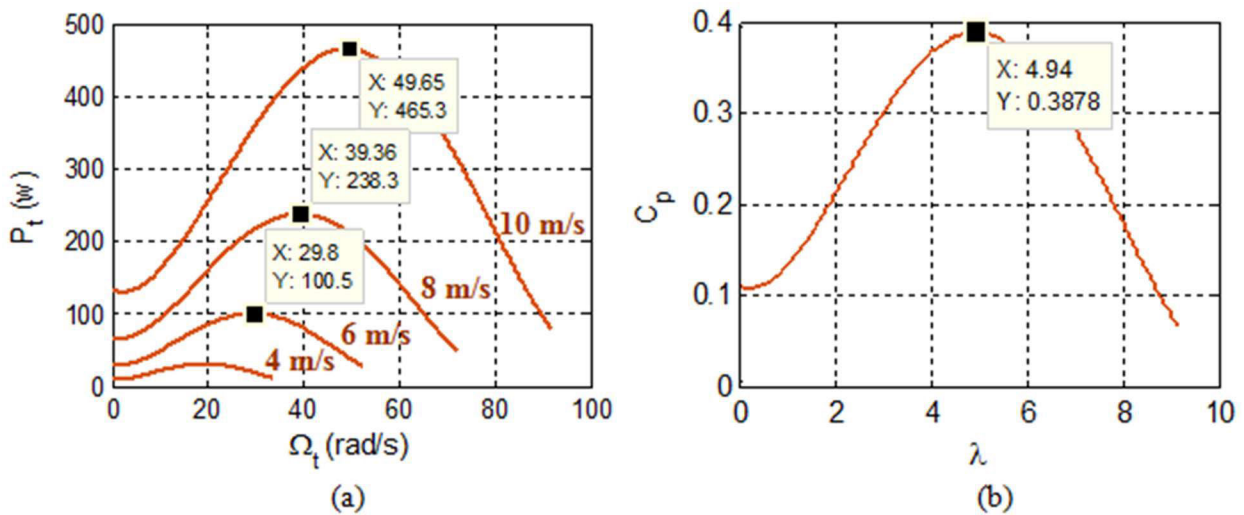


FIGURE 4. WT characteristics: (a) turbine power as a function of rotational speed, (b) power coefficient as a function of relative speed.

a gearbox (Fig. 2). The mechanical coupling between the two systems can be described by (4).

$$J \frac{d\Omega_m}{dt} = T_m - T_e - f\Omega_m \quad (4)$$

With

$$J = \frac{J_t}{G^2} + J_m \quad (5)$$

$$f = \frac{f_t}{G^2} + f_m \quad (6)$$

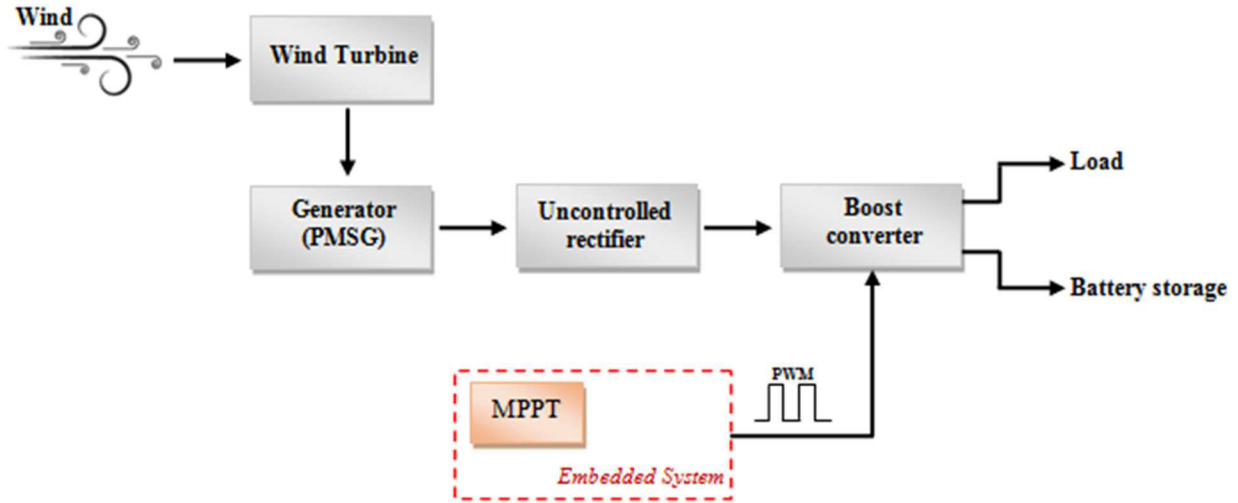


FIGURE 5. Structure of a small power WT chain.

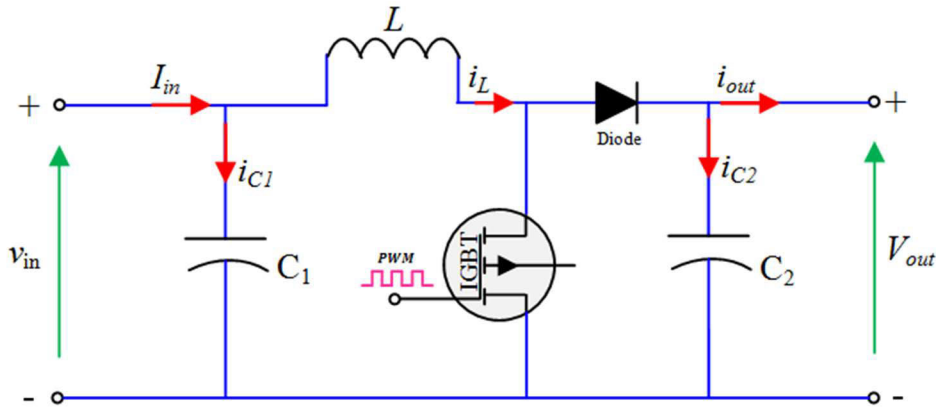


FIGURE 6. Electrical schema of the boost converter.

By modeling the mechanical shaft, it is possible to quantify the real impact of inertia on the dynamics of the WT. Despite the importance of inertia, many researchers [4], [5], [6], [36] did not consider it in their design of WTEs.

The complete model of the WT is illustrated in Fig. 3. The main characteristics describing the aerodynamic behavior of the studied WT are plotted in Fig. 4.

**B. ELECTRICAL PART OF THE WTE**

For the electrical part of the WT, several research works were based on a Permanent Magnet Synchronous Generator (PMSG) connected directly to the WT without the intermediary of a gearbox [10], [11], [14], [24], [26], [37], as illustrated in Fig. 5. This solution has the advantage of being more efficient, with less mechanical losses and low maintenance cost [38], [39], [40]. In addition, a PMSG is characterized by higher efficiency compared to other machines [41], [42]. On the other hand, the main reason in using a DC generator in this work is to reduce the complexity and cost of the designed wind turbine emulator while capturing the behavior of a real

wind turbine. Such a topology which consists of transforming the model of a PMSG and uncontrolled rectifier into an equivalent model of a DC machine has been studied in [43]. Moreover, with a DC generator, the same performance can be achieved as compared to the system (wind turbine + PMSG + uncontrolled rectifier) described in reference [1].

Another important component in the electrical part of the WT system is the power converter. A boost converter was used because of its simple design (Fig. 6) and ease of control which can be easily implemented in practice. This converter is controlled by the MPPT technique so as to force the WT to operate at the optimum power point and also guarantees a better transfer of energy to the electrical load. The operation of the boost converter can be described by the following mathematical model:

$$\begin{cases} \frac{dv_{in}}{dt} = \frac{I_{in}}{C_1} - \frac{i_L}{C_1} \\ \frac{di_L}{dt} = \frac{v_{in}}{L} - (1-d)\frac{V_{out}}{L} \end{cases} \quad (7)$$

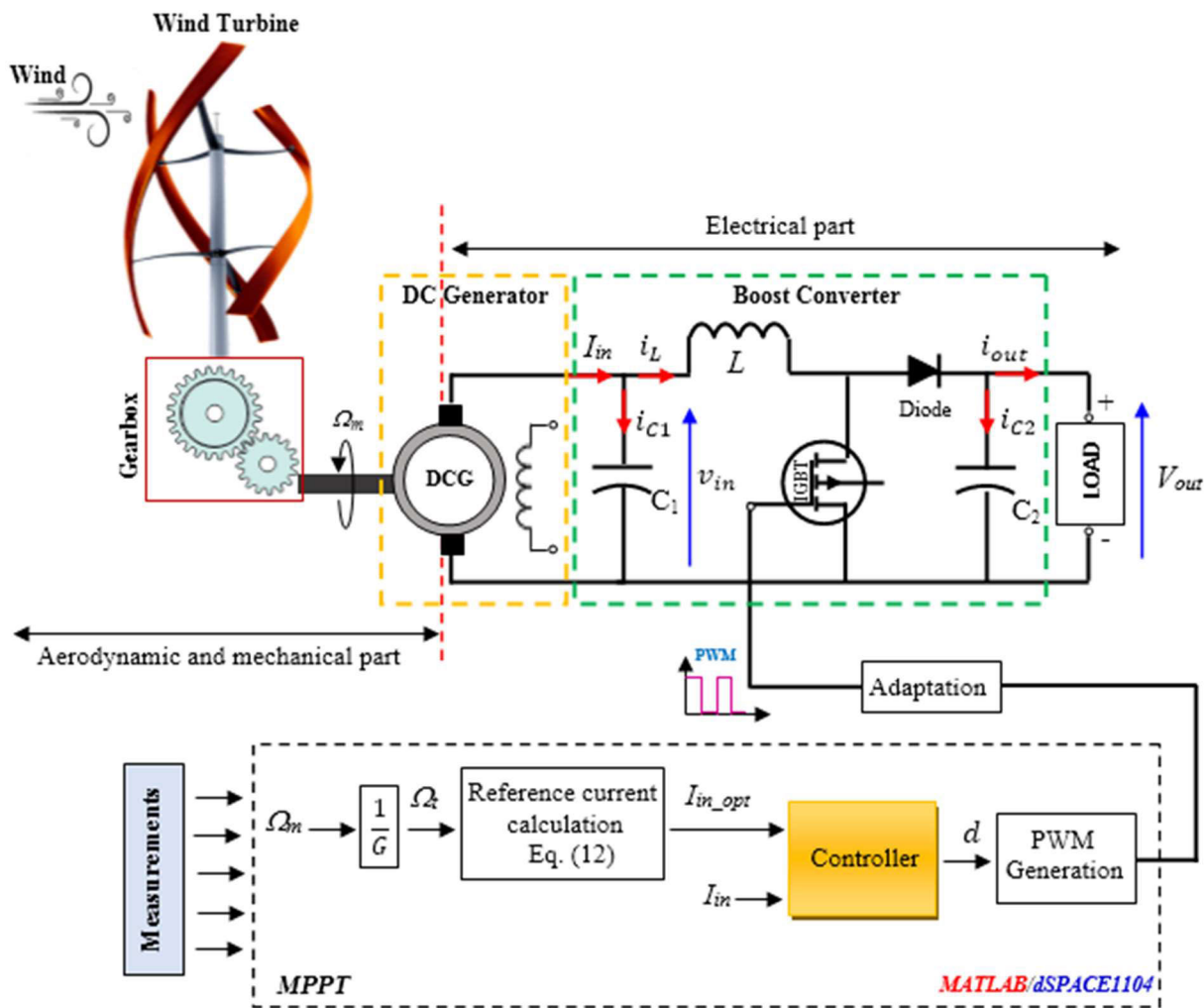


FIGURE 7. Structure adopted for the study of SWTs based on the control of the optimal current as a solution to extract the maximum power from the wind.

where  $v_{in}$  is the input voltage,  $V_{out}$  denotes the output voltage,  $I_{in}$  represents the input current,  $i_L$  is the coil current, and  $d \in [0; 1]$ .

### III. DESIGN OF MPPT

As seen in Fig. 4, the best transfer of aerodynamic energy to the generator (Fig. 4-a) only takes place at the optimum operating point ( $C_{p\_opt} = 0.388$  et  $\lambda_{opt} = 4.94$ ) of the characteristic  $C_p(\lambda)$  of the WT (Fig. 4-b). This is why it is necessary to add MPPT techniques in WT systems. The OTC-MPPT technique used in this work, is simple and easy to implement in practice, but it requires knowledge of the optimal point of the characteristic  $C_p(\lambda)$ , which must be determined beforehand. The operating principle of the OTC method is formulated as follows:

First, the optimal power generated by the WT can be written as follows:

$$P_{t\_opt} = k_{opt} \cdot \Omega_{t\_opt}^3 \tag{8}$$

With

$$k_{opt} = \frac{1}{2} \cdot \frac{C_{p\_opt} \cdot \rho \cdot s \cdot R^3}{\lambda_{opt}^3} \tag{9}$$

The torque relationship that must be imposed on the DCG to help the WT operate at the optimum power point is given by:

$$T_{m\_opt} = \frac{T_{t\_opt}}{G} = \frac{k_{opt}}{G} \cdot \Omega_{t\_opt}^2 \tag{10}$$

Since the torque value can be deduced from the measurement of the current generated by the generator, therefore the torque control is replaced with the current control  $I_{in}$  at the generator output, as shown in Fig. 7. The optimal reference current is calculated as follows:

$$I_{in\_opt} = \frac{T_{m\_opt}}{k} = \frac{k_{opt}}{Gk} \cdot \Omega_{t\_opt}^2 \tag{11}$$

**Note:** The WT that we are going to study in this paper delivers 465.3 w for a wind speed of 10 m/s (test limit), on the other hand, the DC motor used to reproduce the same mechanical

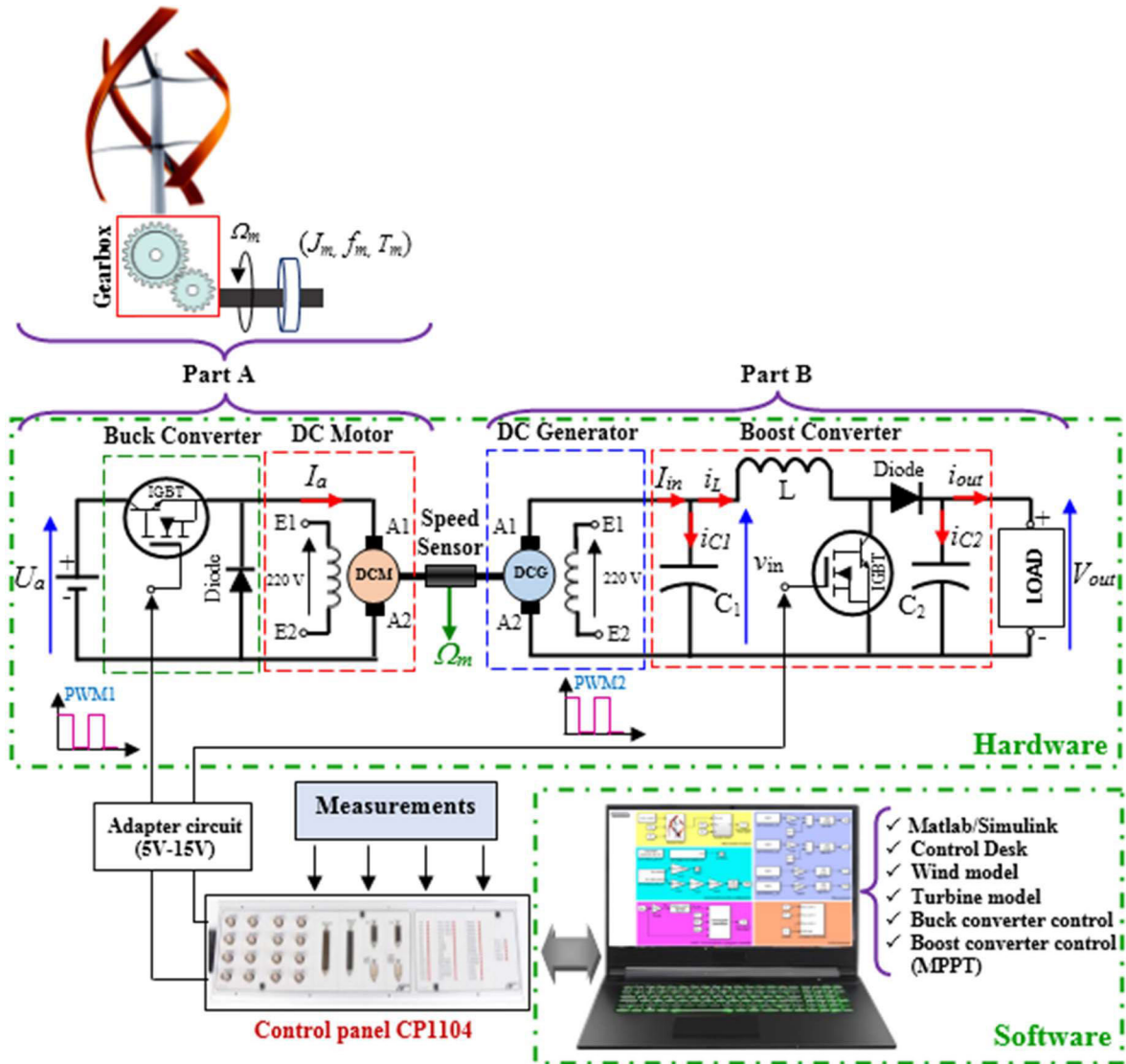


FIGURE 8. Schematic of the principle of the proposed WTE.

behavior as the studied turbine, delivers a nominal power of 100 w. So, to stay within the power limits acceptable by the experimental bench, we decided to apply a ratio of 10 between the power of the WT and the power of the DCM. This power adaptation solution is detailed in reference [9].

So, the optimal current imposed on the DCG becomes:

$$I_{in\_opt} = \frac{k_{opt}}{10 \cdot G \cdot k} \Omega_{r\_opt}^2 \quad (12)$$

Regarding the controllers used in Fig. 7. In this study we have chosen to evaluate the effectiveness of two non-linear controllers; synergetic and backstepping. Hence, a new idea is introduced to control the current at the Boost converter input through these controllers.

### A. SYNERGETIC CONTROLLER

The inputs of the SC are the optimal current  $I_{in\_opt}$  and the measured current  $I_{in}$ . But, the model of the boost converter

given in (7) that we seek to control depends only on the voltage  $v_{in}$  and the coil current  $i_L$ . Therefore, to introduce the term  $I_{in}$  into the model of this converter, the following calculations are performed:

The voltage at the output of the DCG is given by:

$$v_{in} = k\Omega_m - R_a I_{in} \quad (13)$$

So

$$I_{in} = \frac{k\Omega_m}{R_a} - \frac{v_{in}}{R_a} \quad (14)$$

Differentiating (14) with respect to time, gives:

$$\frac{dI_{in}}{dt} = \frac{k\dot{\Omega}_m}{R_a} - \frac{I_{in}}{R_a C_1} + \frac{i_L}{R_a C_1} \quad (15)$$

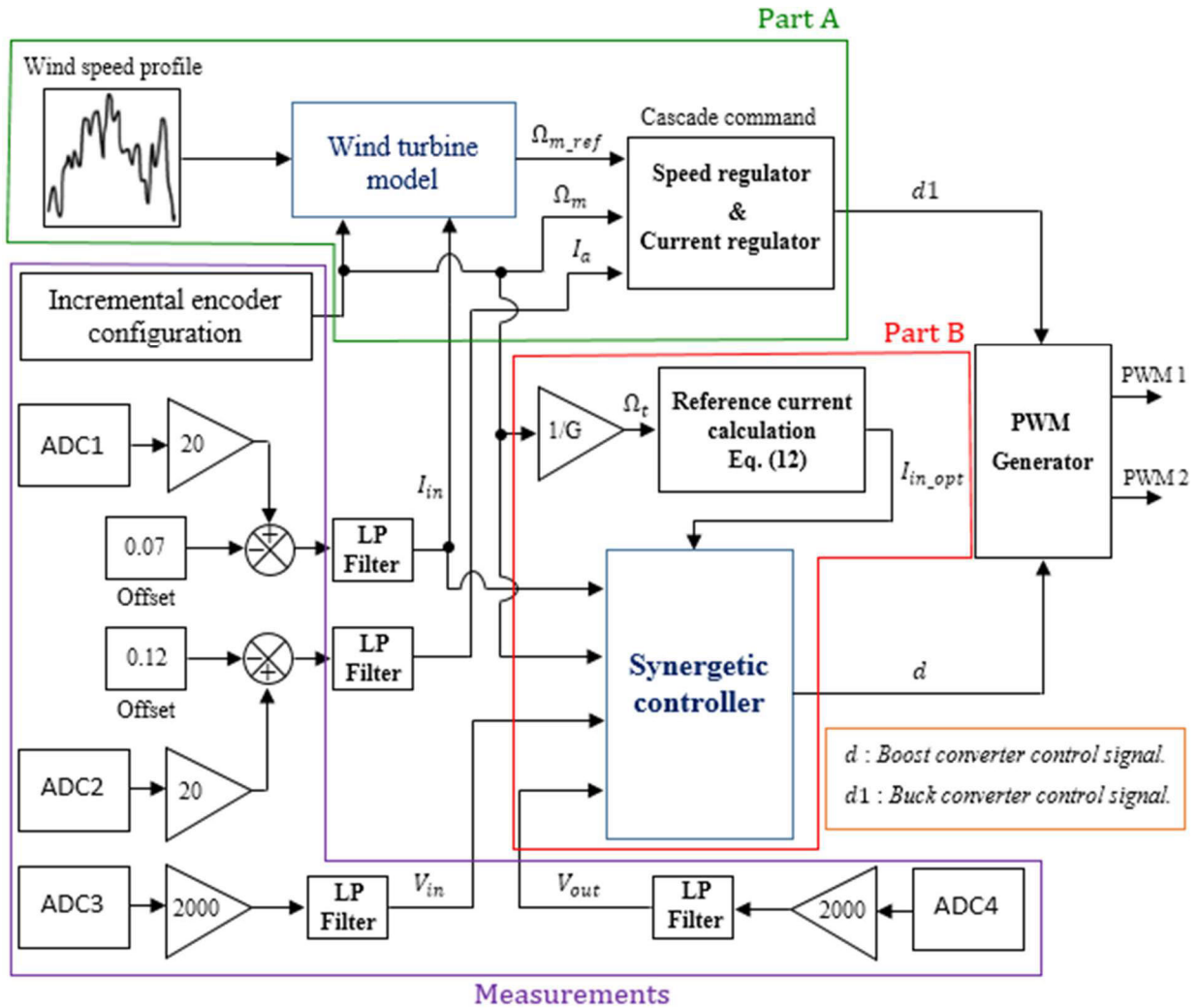


FIGURE 9. The complete experimental diagram adopted for the study of SWTs and the validation of the proposed OTC-MPPT structure (synergetic controller case).

Consider the following system:

$$\begin{cases} \dot{x}_1 = x_2 \\ \dot{x}_2 = \frac{k\ddot{\Omega}_m}{R_a} - \frac{x_2}{R_a C_1} + \frac{v_{in}}{L R_a C_1} - (1-d) \frac{V_{out}}{L R_a C_1} \end{cases} \quad (16)$$

With:  $x_1 = I_{in}$  and  $x_2 = \frac{dI_{in}}{dt}$ .

The first step in synergetic controller design, is the choice of the macro-variable which is given by:

$$\psi = \mu \cdot e + \dot{e} \quad (17)$$

With  $e = I_{in\_opt} - x_1$  and  $\dot{e} = \dot{I}_{in\_opt} - \dot{x}_1$

So

$$\psi = \mu \cdot I_{in\_opt} - \mu x_1 + \dot{I}_{in\_opt} - \dot{x}_1 \quad (18)$$

where  $\mu$  is a large positive constant.

Then, the objective of the synergetic control is to force the macro-variable to converge toward zero using the following convergence law:

$$T \dot{\psi} + \psi = 0 \quad (19)$$

where  $T$  is a positive constant which defines the speed of convergence of the states of the system studied towards the macro-variable.

Differentiating (18) with respect to time leads to:

$$\dot{\psi} = \frac{d\psi}{dt} = \frac{d\psi}{dx} \frac{dx}{dt} = \frac{d\psi}{dx} \dot{x} = \frac{d\psi}{dx_1} \dot{x}_1 + \frac{d\psi}{dx_2} \dot{x}_2 \quad (20)$$

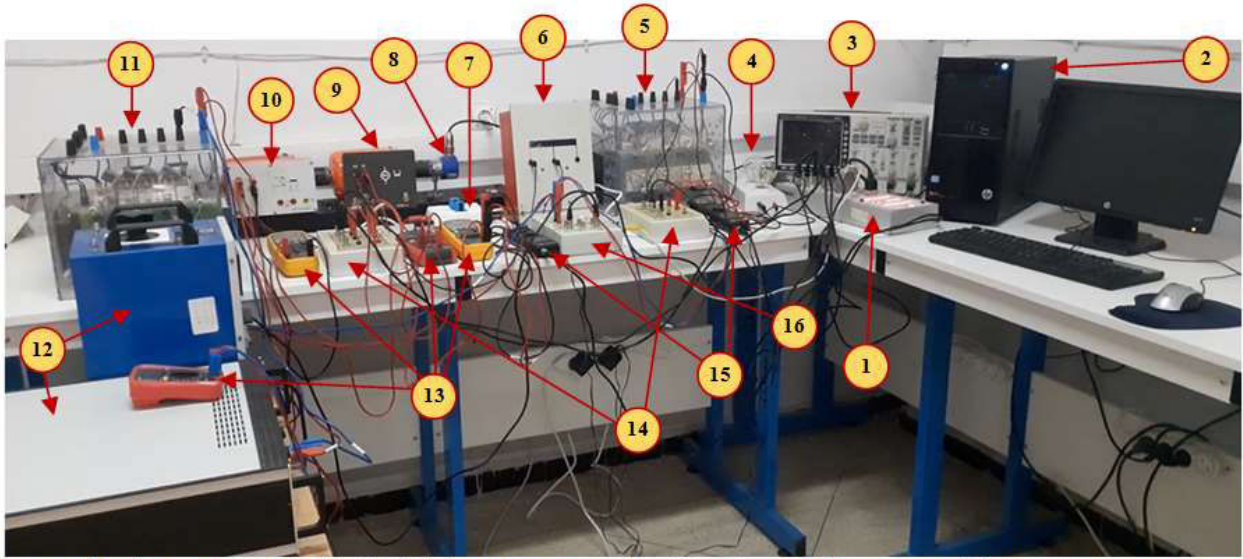
So

$$\dot{\psi} = -\mu \cdot x_2 - \frac{k\ddot{\Omega}_m}{R_a} + \frac{x_2}{R_a C_1} - \frac{v_{in}}{L R_a C_1} + (1-d) \frac{V_{out}}{L R_a C_1} \quad (21)$$

Substituting (21) into (19) and rearranging, leads to the synergetic control law (22).

$$d = 1 - \frac{1}{V_{out}} \left( \frac{-\psi L R_a C_1}{T} + (\mu \cdot L R_a C_1 - L) x_2 + k L C_1 \ddot{\Omega}_m + v_{in} \right) \quad (22)$$

With  $\mu = 20$  and  $T = 0.001$ .



1: Control Panel CP 1104, 2: PC (Matlab/Simulink, dsPACE 1104, control Desk...etc.), 3: Oscilloscope, 4: Load (Lamp1: 220V, 0.4A, 75W & Lamp2: 220V, 0.19A, 40W), 5: DC/DC Boost converter, 6: Input Inductance of Boost converter (L), 7: Input Capacitor of Boost converter (C1), 8: Incremental Encoder, 9: Generator, 10: Motor (wind turbine emulator), 11: DC/DC Buck converter, 12: DC power supply, 13: Multifunction Digital Multimeters ; Voltmeter, Ammeter, Ohmmeter,...etc, 14: Current sensors, 15: Voltage sensors, 16: Adapter circuit (5V-15V).

FIGURE 10. Experimental test bench for the proposed WTE.

### B. BACKSTEPPING CONTROLLER

Consider the following system:

$$\begin{cases} \dot{x}_1 = \frac{k\dot{\Omega}_m}{R_a} - \frac{x_1}{R_a C_1} + \frac{x_2}{R_a C_1} \\ \dot{x}_2 = \frac{v_{in}}{L} - (1-d)\frac{V_{out}}{L} \end{cases} \quad (23)$$

With  $x_1 = I_{in}$  and  $x_2 = i_L$ .

Since the system (23) is of order two, then the backstepping algorithm is carried out in two steps:

- **Step 1** The aim is to regulate the current at the input of the boost converter. Therefore, the first error variable to be defined is given by:

$$e_1 = x_1 - I_{in\_opt} \quad (24)$$

Taking the derivative of (24) with respect to time, gives:

$$\dot{e}_1 = \dot{x}_1 - \dot{I}_{in\_opt} = \frac{k\dot{\Omega}_m}{R_a} - \frac{x_1}{R_a C_1} + \frac{x_2}{R_a C_1} - \dot{I}_{in\_opt} \quad (25)$$

In order to ensure asymptotic stability in the sense of Lyapunov. The following Lyapunov function is used [44]:

$$V(e_1) = \frac{1}{2}e_1^2 \quad (26)$$

Such as

$$\dot{V}(e_1) = e_1 \dot{e}_1 = e_1 \left( \frac{k\dot{\Omega}_m}{R_a} - \frac{x_1}{R_a C_1} + \frac{x_2}{R_a C_1} - \dot{I}_{in\_opt} \right) \quad (27)$$

For asymptotic stability, the Lyapunov function must be positive definite and its time derivative must be negative definite.

Therefore:

$$\begin{aligned} \dot{V}(e_1) = -k_1 e_1^2 = e_1 \left( \frac{k\dot{\Omega}_m}{R_a} - \frac{x_1}{R_a C_1} \right. \\ \left. + \frac{x_2}{R_a C_1} - \dot{I}_{in\_opt} \right) \end{aligned} \quad (28)$$

So

$$-k_1 e_1 = \frac{k\dot{\Omega}_m}{R_a} - \frac{x_1}{R_a C_1} + \frac{x_2}{R_a C_1} - \dot{I}_{in\_opt} \quad (29)$$

Thereafter

$$-k_1 R_a C_1 e_1 = C_1 k \dot{\Omega}_m - x_1 + x_2 - R_a C_1 \dot{I}_{in\_opt} \quad (30)$$

Hence

$$x_2 = \beta = -k_1 R_a C_1 e_1 - C_1 k \dot{\Omega}_m + x_1 + R_a C_1 \dot{I}_{in\_opt} \quad (31)$$

The procedure of backstepping encourages considering  $\beta$  as a first virtual control. Where  $k_1$  is a positive constant.

- **Step 2:** As in the first step, the reference to follow is  $\beta$ . So, the regulation error signal is given by:

$$e_2 = x_2 - \beta \quad (32)$$

Differentiating (32) gives:

$$\dot{e}_2 = \dot{x}_2 - \dot{\beta} = \frac{1}{L} (v_{in} - (1-d)V_{out}) - \dot{\beta} \quad (33)$$

Such as

$$V(e_2) = \frac{1}{2}e_2^2 \quad (34)$$

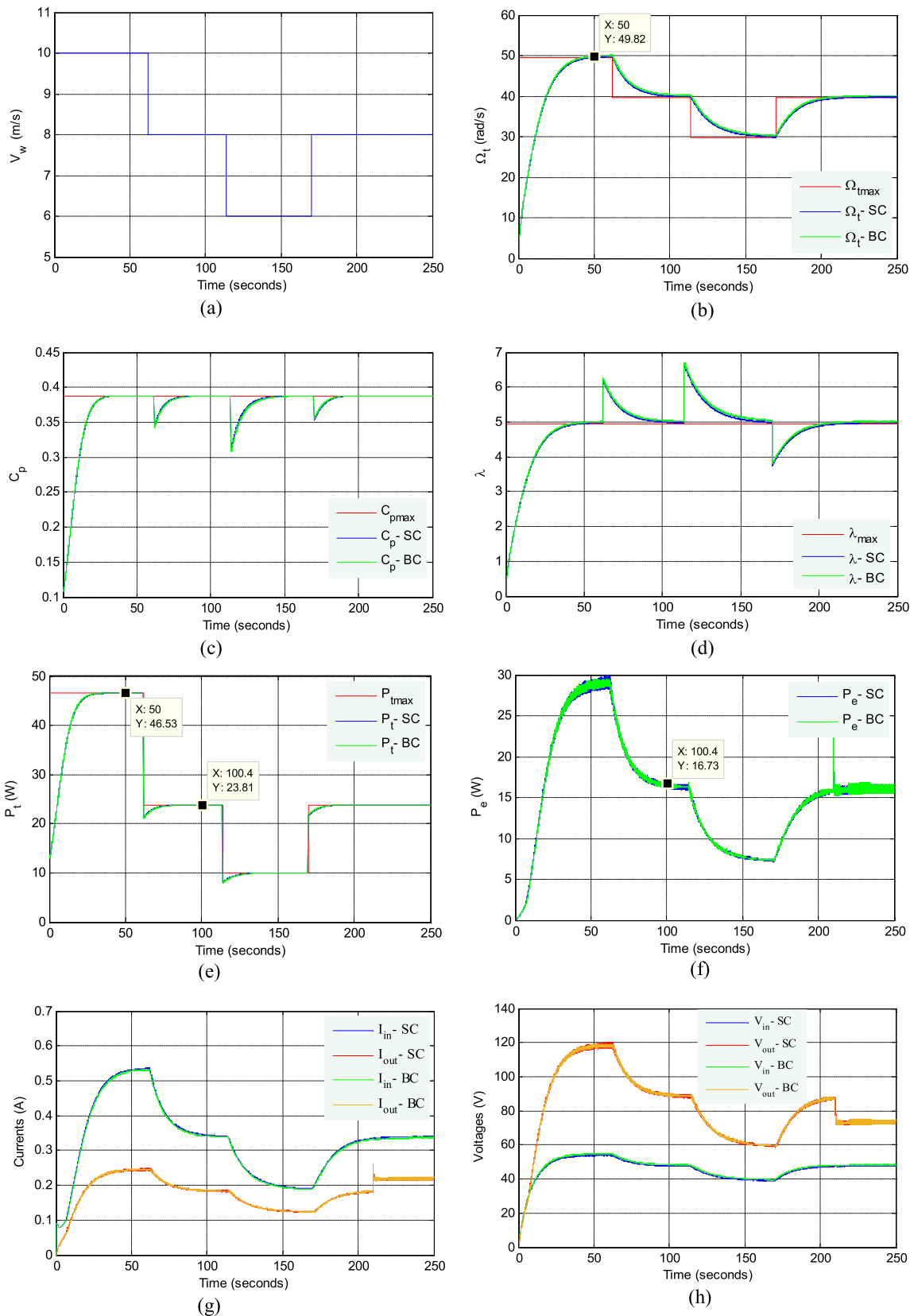


**FIGURE 11.** Experimental results of the first test: (a) wind profile, (b) rotation speed, (c) WT power coefficient, (d) relative speed, (e) WT power, (f) power at the terminals of the electric load, (g) comparison between the current at the input and at the output of the boost converter, (h) comparison between the voltage at the input and at the output of the boost converter, (i) comparison between the optimal current and the current at the input of the boost converter, (j) duty cycle of the DC-DC converter.

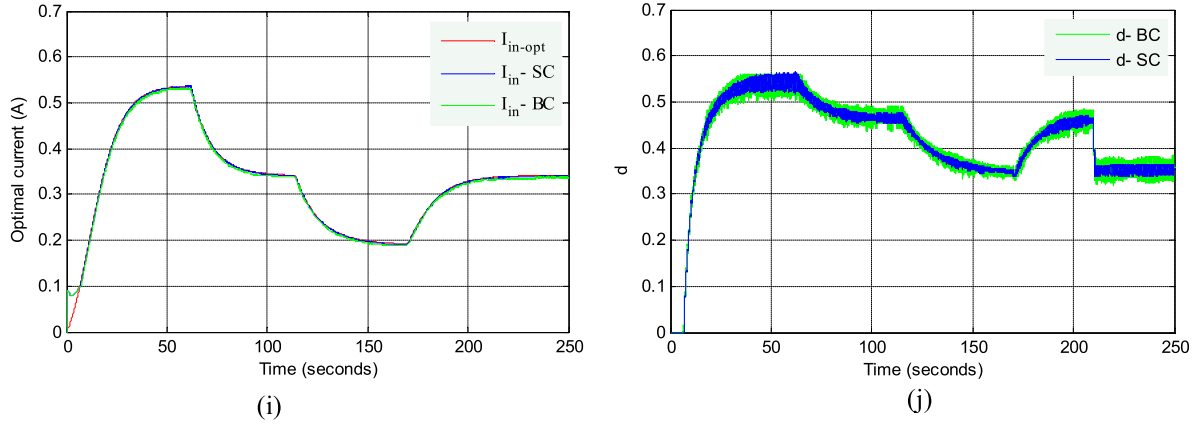


**FIGURE 11. (Continued.)** Experimental results of the first test: (a) wind profile, (b) rotation speed, (c) WT power coefficient, (d) relative speed, (e) WT power, (f) power at the terminals of the electric load, (g) comparison between the current at the input and at the output of the boost converter, (h) comparison between the voltage at the input and at the output of the boost converter, (i) comparison between the optimal current and the current at the input of the boost converter, (j) duty cycle of the DC-DC converter.

Finally, to force the errors  $e_1$  and  $e_2$  converge to zero and ensure the stability of the overall system, the global Lyapunov function is defined as follows:

$$V_t = V(e_1) + V(e_2) \tag{35}$$

The derivative of  $V_t$  is given by:

$$\dot{V}_t = e_1 \dot{e}_1 + e_2 \dot{e}_2 \tag{36}$$

Then

$$\begin{aligned} \dot{e}_1 &= \frac{k\dot{\Omega}_m}{R_a} - \frac{x_1}{R_a C_1} + \frac{1}{R_a C_1}(e_2 + \beta) - \dot{I}_{in\_opt} \\ \dot{e}_1 &= \frac{k\dot{\Omega}_m}{R_a} - \frac{x_1}{R_a C_1} + \frac{e_2}{R_a C_1} + \frac{\beta}{R_a C_1} - \dot{I}_{in\_opt} \\ \dot{e}_1 &= -k_1 e_1 + \frac{e_2}{R_a C_1} \end{aligned} \tag{37}$$

Hence

$$\begin{aligned} \dot{V}_t &= e_1 \left(-k_1 e_1 + \frac{e_2}{R_a C_1}\right) \\ &\quad + e_2 \left(\frac{1}{L}(v_{in} - (1-d)V_{out}) - \dot{\beta}\right) \end{aligned} \tag{38}$$

Or

$$\begin{aligned} \dot{V}_t &= -k_1 e_1^2 + e_2 \left(\frac{e_1}{R_a C_1} + \frac{1}{L}(v_{in} - (1-d)V_{out})\right. \\ &\quad \left.- \dot{\beta}\right) \end{aligned} \tag{39}$$

Thus, for the  $V_t$  function to be positive definite and its time derivative to be negative, the following must hold:

$$-k_2 e_2 = \frac{e_1}{R_a C_1} + \frac{1}{L}(v_{in} - (1-d)V_{out}) - \dot{\beta} \tag{40}$$

where  $k_2$  is a positive constant.

After reducing (40), the backstepping control law is defined as follows:

$$d = 1 + \frac{1}{V_{out}} \left(-Lk_2 e_2 - \frac{L}{R_a C_1} e_1 - v_{in} + L\dot{\beta}\right) \tag{41}$$

The constants are fixed to  $k_1 = 2000$  and  $k_2 = 10$ .

#### IV. EXPERIMENTAL VALIDATION

In order to demonstrate the feasibility and efficiency of the proposed WTE and its ability to reproduce the same mechanical and electrical behavior as a real WT, several experimental tests have been carried out using different wind profiles and electrical loads. Figs. 8, 9 and 10 show the electrical and mechanical parts of the studied WTE, the control schemes, and the components used. The software and hardware parts are briefly described below:

##### A. SOFTWARE PART

So, you can use the software LabVIEW, and LTspice, as you can also use MATLAB/Simulink. In our case, we chose the latter, because it remains simple and gives the possibility of implementing the command model directly on the dSPACE1104 card. Fig. 9 presents a detailed structure of the control scheme of the wind turbine emulator as implemented on the dSPACE board. This figure consists of two main parts: Part A is needed to mimic the mechanical behavior of the wind turbine by controlling the DC motor. The armature of this machine is powered by a Buck-type DC-DC converter. Part B is specific to the OTC-MPPT model used to force the wind turbine to extract the maximum energy from the wind. To operate the system, an ADC block interface is also required to retrieve the measured signals.

##### B. HARDWARE PART

The hardware part is depicted in Fig. 10. The set-up consists of DC power supplies, two DC machines, two DC-DC converters controlled in real-time by the dSPACE1104 board, the electrical load composed of two lamps connected in parallel: Lamp 1: 220 V, 0.4 A, 75 W & Lamp 2: 220 V, 0.19 A, 40 W. Voltage and current measurements are read from voltage and current sensors and an incremental encoder is used to measure the speed of rotation. However, these signals from the sensors contain a lot of noise, and hence low-pass type filters with a cut-off frequency  $\omega_c = 100rad/s$

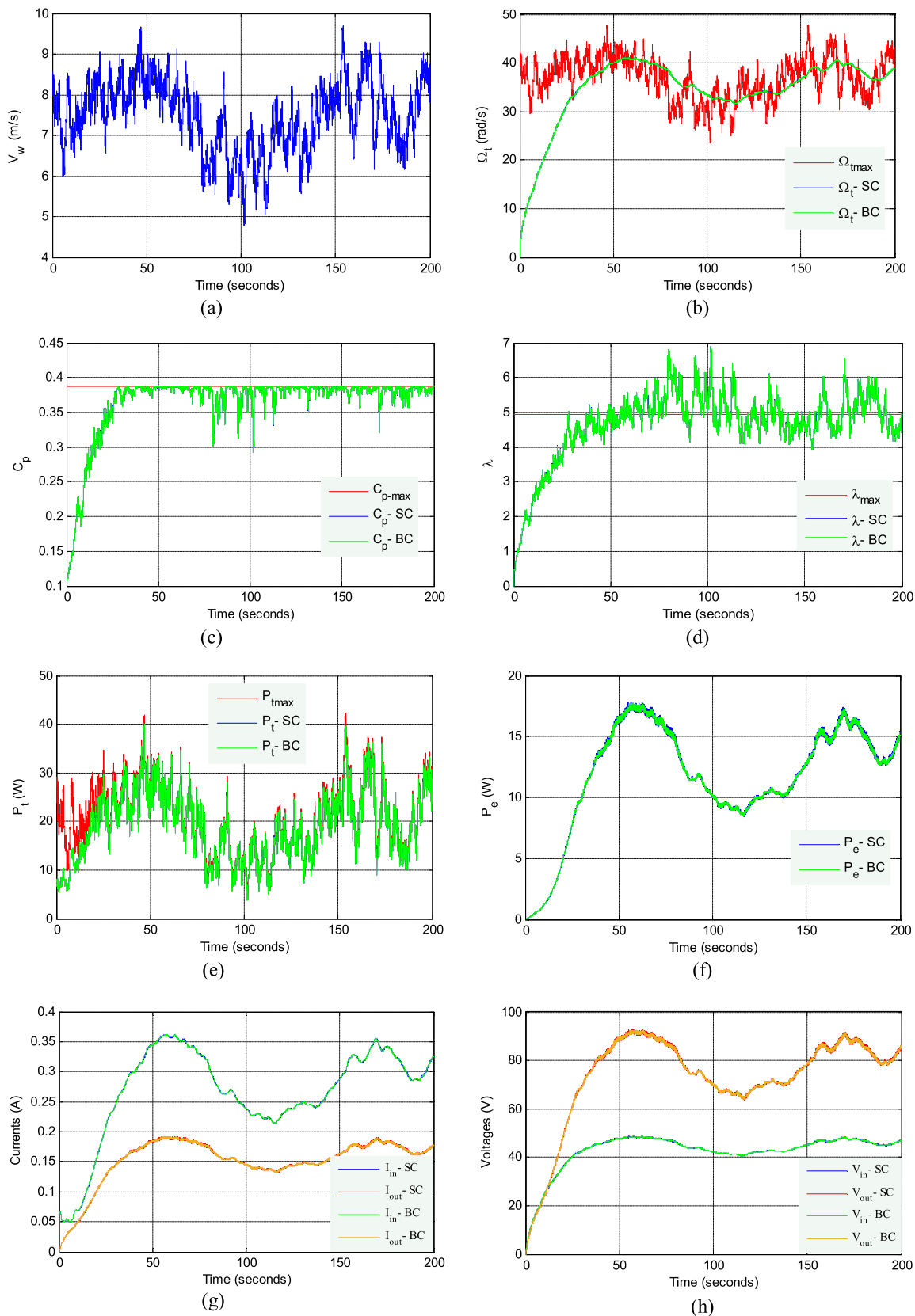


**FIGURE 12.** Experimental results of the second test: (a) wind profile, (b) rotation speed, (c) WT power coefficient, (d) relative speed, (e) WT power, (f) power at the terminals of the electric load, (g) comparison between the current at the input and at the output of the boost converter, (h) comparison between the voltage at the input and at the output of the boost converter, (i) comparison between the optimal current and the current at the input of the boost converter, (j) duty cycle of the DC-DC converter.

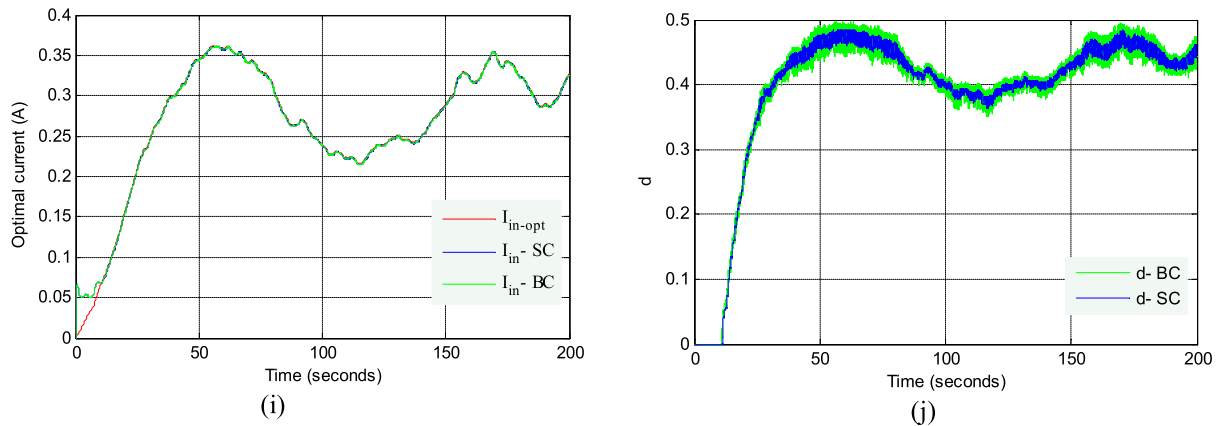


**FIGURE 12. (Continued.)** Experimental results of the second test: (a) wind profile, (b) rotation speed, (c) WT power coefficient, (d) relative speed, (e) WT power, (f) power at the terminals of the electric load, (g) comparison between the current at the input and at the output of the boost converter, (h) comparison between the voltage at the input and at the output of the boost converter, (i) comparison between the optimal current and the current at the input of the boost converter, (j) duty cycle of the DC-DC converter.

are used to guarantee the proper functioning of our WTE and the implemented MPPT technique.

A series of experiments are performed to demonstrate the feasibility of proposed WTE and the effectiveness of the implemented MPPT control technique. They are discussed below:

**Experiment 1:** In this scenario, a wind profile with four consecutive abrupt changes in the wind speed between 6 m/s and 10 m/s, as shown in Fig. (11. a). With this wind profile, we seek to verify the feasibility and efficiency of our WTE to accurately reproduce the same behavior as the real WT studied. We also seek to evaluate the stability, response time, and accuracy of the studied MPPT technique when searching for the optimal points mentioned in Fig. 4. In addition, the robustness of the studied MPPT is also assessed with a variable electrical load. During this experiment, the wind speed set to 8 m/s and at time  $t = 210$  s, the electrical load is varied. In addition, during this test, the effect of the inertia of the turbine is taken into consideration, to demonstrate the influence of this parameter on the operation of the WT and the performance of the MPPT algorithm. The measurements recorded from the sensors are stored in a MATLAB file of type (.mat) from a dSPACE1104 board. The results obtained in this experiment are shown in Fig. 11.

**Experiment 2:** In this experiment, a fixed electrical load consisting of a single connected lamp of 75 W is used and the wind profile was based on a real wind speed as shown in Fig. (12.a) [9] for to get closer to the behavior of a real WT and on the other hand to evaluate the ability of the studied MPPT technique to stabilize the operation of the WT on the point of maximum power despite the turbulent nature of the wind, which includes many oscillations and a lot of noise. The experimental results obtained are shown in Fig. 12.

First of all, although the DC motor used in the design of the WTE is characterized by a nominal power fifteen times less than the nominal power of the turbine studied, we managed to reproduce accurately the same mechanical behavior as the real WT studied. Based on these results, it can be concluded that

the designed WTE works perfectly and remains valid for all types of WTs, regardless of their power.

Furthermore, the MPPT technique studied in this paper showed very good performance under variable wind speeds, hence all the optimal points of (power coefficient, relative speed and turbine power) obtained by simulation (Fig. 4), were accurately reproduced during the experimental tests. For example, for a wind speed of 10 m/s, the maximum power of the turbine is 46.53 W (see Fig. 11.e). If we apply the power adaptation ratio of 1/10, we find the maximum turbine power of about 465.3 W for a rotation speed of 49.82 rad/s (see Fig. 11.b). This good tracking of the maximum power point is observed even in the case of a variable electric load, from where we clearly notice that when we changed the electric load in the time period 210 s and although the wind remains constant during this period, the duty cycle (Fig. 11.j) is decreased to respond to the change in electrical load and also maintains the operation of the WT at the optimum power point.

Thus, from the results of Fig. 11, the significant influence of the inertia of the studied WT can be clearly observed. It generates for each variation of the wind speed a somewhat large response time of around 20 s (similar results were observed in reference [10]). This justifies the delay in the duty cycle response (Fig. 11.j & Fig. 12.j).

Moreover, the low-pass filters used in the control scheme (see Fig. 9), have significantly reduced the noise in the measured signals (voltage, current and rotational speed). With this, we were able to guarantee the proper functioning of our WTE and the proper functioning of the studied MPPT technique. This also allowed us to obtain a good quality of electrical energy produced. Furthermore, between the mechanical power generated by the WT and the electrical power measured at the output of the boost converter, there is a certain difference due to the losses in the machines of the test bench and the losses in the power electronics devices which was not compensated in experimental tests. For example, for a wind speed of 8 m/s, the electrical power

**TABLE 2.** Parameters used during experimental validation.

	Name	Value	Unit
<b>Wind turbine</b>	Nominal power	1.5	kw
	Air density	1.2	kg/m <sup>3</sup>
	Blade radius	1	m
	Height	2	m
	Moment of inertia	5	kg.m <sup>2</sup>
	Coefficient of friction	0.00908	N.m.s/rad
	Maximum power coefficient	0.388	---
	Maximum relative speed	4.94	rad/s
	Multiplication ratio	1.87	---
<b>DC machine</b>	Nominal power	0.1	kw
	Rotor voltage	220	V
	Rotor current	0.63	A
	Rotor resistance	51.47	$\Omega$
	Rotor Inductance	0.2	H
	Stator voltage	220	V
	Stator current	0.08	A
	Nominal speed	2000	rpm
	Moment of inertia	0.0011	kg.m <sup>2</sup>
	Coefficient of friction	0.0002276	N.m.s/rad
	Torque constant	0.891	---
<b>Boost Converter</b>	Input capacitor	10	mF
	Output capacitor	1100	$\mu$ F
	Inductance	50	mH
	Switching frequency	1	kHz

obtained is approximately 16.73 W (see Fig. 11.f). While the mechanical power generated by the WT is equal to 23.81 W (see Fig. 11.e).

On the other hand, the tests carried out with a stochastic wind signal (see Fig. 12.a), confirm the ability of the designed WTE and the proposed MPPT technique studied to operate correctly even under turbulent wind conditions which includes a lot of fluctuation and a lot of noise.

Furthermore, the controllers used alongside the MPPT technique have achieved very good performance for tracking the optimal current reference (see Figs. 11.i and 12.i), whether in terms of speed of response, stability, and precision. In addition, the comparison between the results obtained by the two controllers shows similar performance, except that at the level of the duty cycle signal (see Figs. 11.j and 12.j), the SC has less noise compared to the BC.

## V. CONCLUSION

A new low cost wind emulator has been presented in this work to facilitate the study of small wind turbines. A power maximization strategy based on optimal current control was also validated during this work by different nonlinear controllers.

The results obtained clearly show the feasibility and efficiency of the OTC-MPPT technique and its high performance for maximum power point tracking. The nonlinear controllers used alongside this control strategy provided very good performance for maximum power point tracking. But despite this, the control law obtained by these control techniques (synergetic and/or backstepping) remains a bit complex,

requires prior knowledge of certain system parameters and some parameters that enter into the design of the controller itself. In addition to this, the control signal generated by these control techniques has a lot of noise. On the basis of this study, we see that the advantage of this type of controller does not appear except that they are directly applicable to the nonlinear model of the system that we want to control.

Finally, despite all the obstacles (the permanent absence of wind, the high cost of WTs, etc.) which initially prevented us from carrying out experimental tests on real WTs. In this work, we were able to study it successfully thanks to the proposed WTE. Frankly, this platform has helped us a lot to validate many MPPT techniques without the need to access the real turbines or to know their natural resources. Considering the excellent results obtained, we can say that our WTE remains a very important piece of equipment for teaching and doctoral research at the university. In order to improve this work even more, future work will consider replacing the dSPACE1104 card with a microcontroller-based electronic card (ex: a dsPIC) to reduce more than the cost of designing a WTE. In addition, we are also looking to test another controller alongside the OTC-MPPT which requires fewer measurements and less information on the controlled system, we are talking exactly about the Fuzzy controller. In addition, during the experimental tests carried out in the laboratory, only a resistive variable electrical load was used but the wind emulator can also be connected to other types of loads such as inductive. There are also future plans to synchronize and connect the wind turbine to the electrical network. Thus, test a new diagnostic approach that makes it possible to detect, locate and identify in advance any fault that could alter the operation of the WT or the MPPT algorithm [45], [46].

## APPENDIX

See Table 2.

## ACKNOWLEDGMENT

This work was supported by the Researchers Supporting Project number (RSP2023R258), King Saud University, Riyadh, Saudi Arabia.

## REFERENCES

- [1] H. Boudjemai, S. A. E. M. Ardjoun, H. Chafouk, M. Denai, Z. M. S. Elbarbary, A. I. Omar, and M. M. Mahmoud, "Application of a novel synergetic control for optimal power extraction of a small-scale wind generation system with variable loads and wind speeds," *Symmetry*, vol. 15, no. 2, p. 369, Jan. 2023, doi: [10.3390/sym15020369](https://doi.org/10.3390/sym15020369).
- [2] S. A. E. M. Ardjoun and M. Abid, "Fuzzy sliding mode control applied to a doubly fed induction generator for wind turbines," *TURKISH J. Electr. Eng. Comput. Sci.*, vol. 23, no. 6, pp. 1673–1686, 2015, doi: [10.3906/elk-1404-64](https://doi.org/10.3906/elk-1404-64).
- [3] S. A. E. M. Ardjoun, M. Denai, and M. Abid, "A robust power control strategy to enhance LVRT capability of grid-connected DFIG-based wind energy systems," *Wind Energy*, vol. 22, no. 6, pp. 834–847, Jun. 2019, doi: [10.1002/we.2325](https://doi.org/10.1002/we.2325).
- [4] N. C. Sahoo, A. S. Satpathy, N. K. Kishore, and B. Venkatesh, "D.C. motor-based wind turbine emulator using LabVIEW for wind energy conversion system laboratory setup," *Int. J. Electr. Eng. Educ.*, vol. 50, no. 2, pp. 111–126, Apr. 2013, doi: [10.7227/IJEEE.50.2.1](https://doi.org/10.7227/IJEEE.50.2.1).

- [5] M. A. Bhayo, M. J. A. Aziz, N. R. N. Idris, and A. H. M. Yatim, "Design and development of a wind turbine emulator for analyzing the performance of stand-alone wind energy conversion system," *Int. J. Power Electron. Drive Syst.*, vol. 8, no. 1, pp. 454–461, 2017, doi: [10.11591/ijpeds.v8.i1.pp454-461](https://doi.org/10.11591/ijpeds.v8.i1.pp454-461).
- [6] S. Benzaouia, M. Mokhtari, S. Zouggar, A. Rabhi, M. L. Elhafyani, and T. Ouchbel, "Design and implementation details of a low cost sensorless emulator for variable speed wind turbines," *Sustain. Energy, Grids Netw.*, vol. 26, Jun. 2021, Art. no. 100431, doi: [10.1016/j.segan.2021.100431](https://doi.org/10.1016/j.segan.2021.100431).
- [7] I. Moussa, A. Bouallegue, and A. Khedher, "New wind turbine emulator based on DC machine: Hardware implementation using FPGA board for an open-loop operation," *IET Circuits, Devices Syst.*, vol. 13, no. 6, pp. 896–902, Sep. 2019, doi: [10.1049/iet-cds.2018.5530](https://doi.org/10.1049/iet-cds.2018.5530).
- [8] M. E. Abdallah, O. M. Arafa, A. Shaltot, and G. A. A. Aziz, "Wind turbine emulation using permanent magnet synchronous motor," *J. Electr. Syst. Inf. Technol.*, vol. 5, no. 2, pp. 121–134, Sep. 2018, doi: [10.1016/j.jesit.2018.03.005](https://doi.org/10.1016/j.jesit.2018.03.005).
- [9] H. Boudjemai, S. A. M. Ardjoun, H. Chafouk, and M. Denai, "Design and experimental validation for a small wind turbine emulator," in *Proc. 2nd Int. Conf. Electron. Elect. Eng. (ICE)*, Bouira, Algeria, Nov. 2020, pp. 1–6.
- [10] R. Aubrée, F. Auger, M. Macé, and L. Loron, "Design of an efficient small wind-energy conversion system with an adaptive sensorless MPPT strategy," *Renew. Energy*, vol. 86, pp. 280–291, Feb. 2016, doi: [10.1016/j.renene.2015.07.091](https://doi.org/10.1016/j.renene.2015.07.091).
- [11] İ. Yazıcı and E. K. Yaylacı, "Improving efficiency of the tip speed ratio-MPPT method for wind energy systems by using an integral sliding mode voltage regulator," *J. Energy Resour. Technol.*, vol. 140, no. 5, May 2018, doi: [10.1115/1.4038485](https://doi.org/10.1115/1.4038485).
- [12] M. M. Mahmoud, B. S. Atia, Y. M. Esmail, S. A. E. M. Ardjoun, N. Anwer, A. I. Omar, F. Alsaif, S. Alsulamy, and S. A. Mohamed, "Application of whale optimization algorithm based FOPI controllers for STATCOM and UPQC to mitigate harmonics and voltage instability in modern distribution power grids," *Axioms*, vol. 12, no. 5, p. 420, Apr. 2023, doi: [10.3390/axioms12050420](https://doi.org/10.3390/axioms12050420).
- [13] M.-F. Tsai, C.-S. Tseng, and Y.-H. Hung, "A novel MPPT control design for wind-turbine generation systems using neural network compensator," in *Proc. 38th Annu. Conf. IEEE Ind. Electron. Soc. (IECON)*, Oct. 2012, pp. 3521–3526, doi: [10.1109/IECON.2012.6389333](https://doi.org/10.1109/IECON.2012.6389333).
- [14] M. A. Abdullah, A. H. M. Yatim, C. W. Tan, and R. Saidur, "A review of maximum power point tracking algorithms for wind energy systems," *Renew. Sustain. Energy Rev.*, vol. 16, no. 5, pp. 3220–3227, Jun. 2012, doi: [10.1016/j.rser.2012.02.016](https://doi.org/10.1016/j.rser.2012.02.016).
- [15] J. C. Mayo-Maldonado, R. Salas-Cabrera, H. Cisneros-Villegas, R. Castillo-Ibarra, J. Roman-Flores, and M. A. Hernandez-Colin, "Maximum power point tracking control for a DC-generator/multiplier-converter combination for wind energy applications," in *Proc. World Congr. Eng. Comput. Sci. (WCECS)*, San Francisco, CA, USA, vol. 1, Oct. 2011, pp. 19–21.
- [16] M. Karabacak, "A new perturb and observe based higher order sliding mode MPPT control of wind turbines eliminating the rotor inertial effect," *Renew. Energy*, vol. 133, pp. 807–827, Apr. 2019, doi: [10.1016/j.renene.2018.10.079](https://doi.org/10.1016/j.renene.2018.10.079).
- [17] C. I. Martínez-Márquez, J. D. Twizere-Bakunda, D. Lundback-Mompó, S. Orts-Grau, F. J. Gimeno-Sales, and S. Seguí-Chilet, "Small wind turbine emulator based on lambda-cp curves obtained under real operating conditions," *Energies*, vol. 12, no. 13, p. 2456, Jun. 2019, doi: [10.3390/en12132456](https://doi.org/10.3390/en12132456).
- [18] Y. E. A. Eldahab, N. H. Saad, and A. Zekry, "Assessing wind energy conversion systems based on newly developed wind turbine emulator," *Int. J. Smart Grid*, vol. 4, no. 4, pp. 136–148, 2020, doi: [10.20508/ijsmartgrid.v4i4.133.g101](https://doi.org/10.20508/ijsmartgrid.v4i4.133.g101).
- [19] K. Premkumar, M. Vishnupriya, T. S. Babu, B. V. Manikandan, T. Thamizhselvan, A. N. Ali, M. R. Islam, A. Z. Kouzani, and M. A. P. Mahmud, "Black widow optimization-based optimal PI-controlled wind turbine emulator," *Sustainability*, vol. 12, no. 24, p. 10357, Dec. 2020, doi: [10.3390/su122410357](https://doi.org/10.3390/su122410357).
- [20] A. Hazzab, H. Gouabi, M. Habbab, M. Rezkallah, H. Ibrahim, and A. Chandra, "Wind turbine emulator control improvement using nonlinear PI controller for wind energy conversion system: Design and real-time implementation," *Int. J. Adapt. Control Signal Process.*, vol. 37, no. 5, pp. 1151–1165, May 2023, doi: [10.1002/acs.3566](https://doi.org/10.1002/acs.3566).
- [21] S. M. Barakati, M. Kazerani, and J. D. Aplevich, "Maximum power tracking control for a wind turbine system including a matrix converter," *IEEE Trans. Energy Convers.*, vol. 24, no. 3, pp. 705–713, Sep. 2009, doi: [10.1109/TEC.2008.2005316](https://doi.org/10.1109/TEC.2008.2005316).
- [22] X. Deng, J. Yang, Y. Sun, D. Song, Y. Yang, and Y. H. Joo, "An effective wind speed estimation based extended optimal torque control for maximum wind energy capture," *IEEE Access*, vol. 8, pp. 65959–65969, 2020, doi: [10.1109/ACCESS.2020.2984654](https://doi.org/10.1109/ACCESS.2020.2984654).
- [23] M. Yin, W. Li, C. Y. Chung, L. Zhou, Z. Chen, and Y. Zou, "Optimal torque control based on effective tracking range for maximum power point tracking of wind turbines under varying wind conditions," *IET Renew. Power Gener.*, vol. 11, no. 4, pp. 501–510, Mar. 2017, doi: [10.1049/iet-rpg.2016.0635](https://doi.org/10.1049/iet-rpg.2016.0635).
- [24] R. I. Putri, M. Pujiantara, A. Priyadi, T. Ise, and M. H. Purnomo, "Maximum power extraction improvement using sensorless controller based on adaptive perturb and observe algorithm for PMSG wind turbine application," *IET Electr. Power Appl.*, vol. 12, no. 4, pp. 455–462, Apr. 2018, doi: [10.1049/iet-epa.2017.0603](https://doi.org/10.1049/iet-epa.2017.0603).
- [25] K. Belmokhtar, M. L. Doumbia, and K. Agbossou, "Novel fuzzy logic based sensorless maximum power point tracking strategy for wind turbine systems driven DFIG (doubly-fed induction generator)," *Energy*, vol. 76, pp. 679–693, Nov. 2014, doi: [10.1016/j.energy.2014.08.066](https://doi.org/10.1016/j.energy.2014.08.066).
- [26] H. Sefidgar and S. A. Gholamian, "Fuzzy logic control of wind turbine system connection to PM synchronous generator for maximum power point tracking," *Int. J. Intell. Syst. Appl.*, vol. 6, no. 7, pp. 29–35, Jun. 2014, doi: [10.5815/ijisa.2014.07.04](https://doi.org/10.5815/ijisa.2014.07.04).
- [27] J.-H. Chen, H.-T. Yau, and W. Hung, "Design and study on sliding mode extremum seeking control of the chaos embedded particle swarm optimization for maximum power point tracking in wind power systems," *Energies*, vol. 7, no. 3, pp. 1706–1720, Mar. 2014, doi: [10.3390/en7031706](https://doi.org/10.3390/en7031706).
- [28] Y. S. Hagh, A. Fekih, and H. Handroos, "Robust PI-based non-singular terminal synergetic control for nonlinear systems via hybrid nonlinear disturbance observer," *IEEE Access*, vol. 9, pp. 97401–97414, 2021, doi: [10.1109/ACCESS.2021.3094554](https://doi.org/10.1109/ACCESS.2021.3094554).
- [29] H. Benbouhenni and N. Bizon, "Terminal synergetic control for direct active and reactive powers in asynchronous generator-based dual-rotor wind power systems," *Electronics*, vol. 10, no. 16, p. 1880, Aug. 2021, doi: [10.3390/electronics10161880](https://doi.org/10.3390/electronics10161880).
- [30] A. Ardjal, M. Bettayeb, and R. Mansouri, "Fractional nonlinear synergetic control of wind turbine for maximum power point tracking," in *Proc. IEEE Int. Symp. Signal Process. Inf. Technol. (ISSPIT)*, Dec. 2019, pp. 1–6, doi: [10.1109/ISSPIT47144.2019.9001862](https://doi.org/10.1109/ISSPIT47144.2019.9001862).
- [31] N. Zerroug, M. N. Harmas, S. Benagoune, Z. Bouchama, and K. Zehar, "DSP-based implementation of fast terminal synergetic control for a DC-DC buck converter," *J. Franklin Inst.*, vol. 355, no. 5, pp. 2329–2343, Mar. 2018, doi: [10.1016/j.jfranklin.2018.01.004](https://doi.org/10.1016/j.jfranklin.2018.01.004).
- [32] A. T. Azar, F. E. Serrano, M. A. Flores, S. Vaidyanathan, and Q. Zhu, "Adaptive neural-fuzzy and backstepping controller for port-Hamiltonian systems," *Int. J. Comput. Appl. Technol.*, vol. 62, no. 1, pp. 1–12, 2020.
- [33] A. V. Gulalkari, P. S. Pratama, G. Hoang, D. H. Kim, B. H. Jun, and S. B. Kim, "Object tracking and following six-legged robot system using Kinect camera based on Kalman filter and backstepping controller," *J. Mech. Sci. Technol.*, vol. 29, no. 12, pp. 5425–5436, Dec. 2015, doi: [10.1007/s12206-015-1144-4](https://doi.org/10.1007/s12206-015-1144-4).
- [34] J. R. Azinheira, A. Moutinho, and E. C. de Paiva, "A backstepping controller for path-tracking of an underactuated autonomous airship," *Int. J. Robust Nonlinear Control, IFAC-Affiliated J.*, vol. 19, no. 4, pp. 418–441, Mar. 2009, doi: [10.1002/rnc.1325](https://doi.org/10.1002/rnc.1325).
- [35] Y. Xia, M. Fu, P. Shi, Z. Wu, and J. Zhang, "Adaptive backstepping controller design for stochastic jump systems," *IEEE Trans. Autom. Control*, vol. 54, no. 12, pp. 2853–2859, Dec. 2009, doi: [10.1109/TAC.2009.2033131](https://doi.org/10.1109/TAC.2009.2033131).
- [36] F. Martínez, L. C. Herrero, and S. de Pablo, "Open loop wind turbine emulator," *Renew. Energy*, vol. 63, pp. 212–221, Mar. 2014, doi: [10.1016/j.renene.2013.09.019](https://doi.org/10.1016/j.renene.2013.09.019).
- [37] K. Kumar, N. Ramesh Babu, and K. R. Prabhu, "Design and analysis of RBFN-based single MPPT controller for hybrid solar and wind energy system," *IEEE Access*, vol. 5, pp. 15308–15317, 2017, doi: [10.1109/ACCESS.2017.2733555](https://doi.org/10.1109/ACCESS.2017.2733555).
- [38] Y. Kim, M. Kang, E. Muljadi, J.-W. Park, and Y. C. Kang, "Power smoothing of a variable-speed wind turbine generator in association with the rotor-speed-dependent gain," *IEEE Trans. Sustain. Energy*, vol. 8, no. 3, pp. 990–999, Jul. 2017, doi: [10.1109/TSSTE.2016.2637907](https://doi.org/10.1109/TSSTE.2016.2637907).
- [39] C. Wei, Z. Zhang, W. Qiao, and L. Qu, "An adaptive network-based reinforcement learning method for MPPT control of PMSG wind energy conversion systems," *IEEE Trans. Power Electron.*, vol. 31, no. 11, pp. 7837–7848, Nov. 2016, doi: [10.1109/TPEL.2016.2514370](https://doi.org/10.1109/TPEL.2016.2514370).

[40] M. E. Haque, M. Negnevitsky, and K. M. Muttaqi, "A novel control strategy for a variable-speed wind turbine with a permanent-magnet synchronous generator," in *Proc. IEEE Ind. Appl. Soc. Annu. Meeting*, Nov. 2008, pp. 1–8, doi: [10.1109/TIA.2009.2036550](https://doi.org/10.1109/TIA.2009.2036550).

[41] A. D. Hansen and G. Michalke, "Modelling and control of variable speed multi-pole permanent magnet synchronous generator wind turbine," *Wind Energy, Int. J. Prog. Appl. Wind Power Convers. Technol.*, vol. 11, no. 5, pp. 537–554, 2008, doi: [10.1002/we.278](https://doi.org/10.1002/we.278).

[42] F. Deng, D. Liu, Z. Chen, and P. Su, "Control strategy of wind turbine based on permanent magnet synchronous generator and energy storage for stand-alone systems," *Chin. J. Electr. Eng.*, vol. 3, no. 1, pp. 51–62, 2017, doi: [10.23919/CJEE.2017.7961322](https://doi.org/10.23919/CJEE.2017.7961322).

[43] B. Sareni, A. Abdelli, X. Roboam, and D. H. Tran, "Model simplification and optimization of a passive wind turbine generator," *Renew. Energy*, vol. 34, no. 12, pp. 2640–2650, Dec. 2009, doi: [10.1016/j.renene.2009.04.024](https://doi.org/10.1016/j.renene.2009.04.024).

[44] S. A. E. M. Ardjoun, M. Denai, and H. Chafouk, "A robust control approach for frequency magnet support capability of grid-tie photovoltaic systems," *J. Sol. Energy Eng.*, vol. 145, no. 2, Apr. 2023, Art. no. 021009, doi: [10.1115/1.4055099](https://doi.org/10.1115/1.4055099).

[45] L. I. Gliga, H. Chafouk, D. Popescu, and C. Lupu, "Diagnosis of a permanent magnet synchronous generator using the extended Kalman filter and the fast Fourier transform," in *Proc. 7th Int. Conf. Syst. Control (ICSC)*, Oct. 2018, pp. 65–70, doi: [10.1109/ICoSc.2018.8587632](https://doi.org/10.1109/ICoSc.2018.8587632).

[46] S. A. E. M. Ardjoun, M. Denai, and M. Abid, "Robustification du contrôle des éoliennes pour une meilleure intégration dans un réseau déséquilibré," in *Proc. Algerian Large Elect. Netw. Conf. (CAGRE)*, Algiers, Algeria, 2019, pp. 1–6, doi: [10.1109/CAGRE.2019.8713286](https://doi.org/10.1109/CAGRE.2019.8713286).



**MOULOUD DENAI** received the joint Graduate degree in electrical engineering from the University of Science and Technology of Algiers and École Nationale Polytechnique of Algiers, Algeria, and the Ph.D. degree in control engineering from The University of Sheffield, U.K. He was with the University of Science and Technology of Oran, Algeria, until 2004. From 2004 to 2010, he was with The University of Sheffield. From 2010 to 2014, he was with the University of Teesside, U.K. Since 2014, he has been with the University of Hertfordshire, U.K. His research interests include modeling, optimization, and control of engineering and life science (biological and biomedical) systems. His current research interests include energy include intelligent control design and computational intelligence applications to efficiency optimization in renewable energy systems, with a particular focus on the management of smart homes and dynamic scheduling, optimization and control of future smart grids, condition monitoring and asset management in electric power networks, energy storage systems integration into the grid, smart meter data analytics using machine learning techniques for efficient energy management, electric vehicles integration into the distribution grid, and V2G/G2V management.



**ABDULAZIZ ALKUHAyli** (Member, IEEE) received the B.Sc. degree in electrical engineering from King Saud University, Riyadh, Saudi Arabia, in 2006, the M.S. degree in electrical engineering from the Missouri University of Science and Technology, Rolla, MO, USA, in 2013, and the Ph.D. degree in electrical engineering from North Carolina State University, Raleigh, NC, USA, in 2018. From 2006 to 2009, he was an Operation Engineer with the Energy Control Center, Saudi Electricity Company. He is currently an Assistant Professor with the Department of Electrical Engineering, King Saud University. His research interests include energy management, renewable energy systems, flexible AC transmission systems, power system stability, and smart grids.



**USAMA KHALED** received the M.Sc. degree in electrical engineering from Aswan University, Egypt, in 1998 and 2003, respectively, and the joint Ph.D. degree in electrical engineering from Cairo University, Egypt, and Kyushu University, Japan, through a Joint Scholarship, in 2010. Since 2000, he has been with the Department of Electrical Power Engineering, Faculty of Energy Engineering, Aswan University, Egypt. His research interests include nano-dielectric materials, applied electrostatics, renewable energy, and high voltage technologies. He has been an Assistant Professor and an Associate Professor with the College of Engineering, King Saud University, since 2014 and 2018, respectively. He is currently a Professor and the Head of the Electrical Engineering Department, Faculty of Engineering, Aswan University.



**MOHAMED METWALLY MAHMOUD** was born in Sohag, Egypt. He received the B.Sc., M.Sc., and Ph.D. degrees in electrical engineering from Aswan University, Egypt, in 2015, 2019, and 2022, respectively. He is currently a Professor (Assistant) with Aswan University. His research interests include performance improvement of wind generators, optimization methods, intelligent controllers, fault ride-through capability, power quality, FACTS tools, and energy storage systems. He has been awarded Aswan University prizes for international publishing, in 2020, 2021, and 2022, respectively. He is the author or coauthor of many refereed journals and conference papers. He reviews for all well-known publishers (IEEE, Springer, Wiley, Elsevier, Taylor & Francis, Sage, and Hindawi).



**HAMZA BOUDJEMAI** was born in Tlemcen, Algeria, in July 1994. He received the master's degree in electrical control from the University of Tlemcen, Algeria, in 2018. He is currently pursuing the Ph.D. degree with the Electrical Engineering Department, Djillali Liabes University, Algeria. His primary research interests include advanced control and fault diagnosis in renewable energy domain.



**SID AHMED EL MEHDI ARDJOUN** received the State Engineering, Magister, Doctorate of Science, and H.D.R. degrees in electrical engineering (option: electrical control and electromechanical converters) from Djillali Liabes University, Algeria, in 2008, 2010, 2016, and 2019, respectively. Since 2010, he has been with the IRECOM Laboratory as a Researcher and since 2013, he has been with the Faculty of Electrical Engineering as a Lecturer. His research interests include electric control (robust control, intelligent control, and fault tolerant control) in renewable energy and electric drives domain.



**HOUCINE CHAFOUK** received the M.S. and Ph.D. degrees in automatic control from the University of Nancy, Nancy, France, in 1986 and 1990, respectively. Then, he joined the Graduate School of Electrical Engineering, ESIGELEC, Rouen, France. From 2000 to 2008, he was the Leader of the Automatics Control and Systems Research Team and the Research Head of ESIGELEC. He is currently with IRSEEM/ ESIGELEC, Normandy University of Rouen, France. From 2000 to 2018, he was the coauthor of 115 research papers in the areas of advanced control systems, fault tolerant control and fault diagnosis applied to renewal energy, and automotive and aerospace fields.